



**Repositorio Institucional de la Universidad Autónoma de Madrid**

<https://repositorio.uam.es>

Esta es la **versión de autor** del artículo publicado en:

This is an **author produced version** of a paper published in:

IEEE Transactions on Nanotechnology 12.2 (2013): 152 – 156

**DOI:** <http://dx.doi.org/10.1109/TNANO.2012.2235081>

**Copyright:** © 2013 IEEE

El acceso a la versión del editor puede requerir la suscripción del recurso

Access to the published version may require subscription

# Influence of the Substrate and Tip Shape on the Characterization of Thin Films by Electrostatic Force Microscopy.

G. M. Sacha

**Abstract**—Electrostatic force microscopy has been shown to be a useful tool to determine the dielectric constant of nanoscaled thin films that play a key role in many electrical, optical and biological phenomena. Previous approaches have made use of simple analytical models to analyze the experimental data for these materials. Here we show that the electrostatic force shows a completely different behavior when the shape of the tip and sample are taken into account. We present a complete study of the interaction between the whole tip and the layers below the thin film. We demonstrate that physical magnitudes such as the surface charge density distribution and the size of the materials have a strong influence on the EFM signal. The EFM sensitivity to the substrate below the thin film decreases with the substrate thickness and saturates for thicknesses above two times the length of the tip, when it is close to that of an infinite medium.

**Index Terms** – Electrostatic Force Microscopy, Thin Films

## I. INTRODUCTION

By applying a voltage between a force microscope tip and a sample, electrostatic force microscopy[1] (EFM) has succeeded in the analysis of different materials[2], [3], [4], [5], [6], [7] at the nanoscale. However, the understanding and simulation of the tip-sample interaction requires a great effort for the users due to the long-range nature of the electrostatic force. Because of that, it has been demonstrated that most of the elements of the EFM setup must be included in the numerical simulations for a quantitative characterization of the materials.[8] Moreover, it has been demonstrated that the use of dielectric substrates produces complex interactions between the sample and the shape of the tip (including the cantilever).[9] In the case of thin films, it has been also shown that the substrate thickness and dielectric constant are key parameters for a quantitative characterization.[10] Some effects like the detection of effective ultrahigh dielectric constants due, for example, to the presence of certain conductivity in the thin film can be also present. [11] In the EFM setup proposed in this article, there are at least three layers that could modify the magnitude and behaviour of the electrostatic force.

The main problem of numerical simulations that involve many EFM elements is that the tip-sample distance is at least three orders of magnitude smaller than other magnitudes such as the tip length or the substrate thickness. To overcome this

problem, thin film samples have been simulated by simplifying the geometry[12] or restricting parameters such as the dielectric constant of the substrate[13]. In most of the cases, these approximations are not good enough for a correct quantitative characterization or do not reproduce the correct experimental setup. In this article, we will make a complete analysis of the electrostatic interaction in an EFM setup that includes elements that may have a strong influence on the signal. First, we will simulate a structure formed by three layers: a dielectric thin film, a dielectric substrate and a grounded metallic plate, which is a common experimental setup in the imaging and characterization of thin films. The long-range nature of the electrostatic force makes us analyse also the relation between the shape of the tip and all the parameters of the sample. Second, we will compare the results of the whole geometry with results obtained with spherical tips, trying to establish how good the spherical tip is as a model for the EFM simulation. We will show that, for some particular EFM geometries, spherical tip gives quantitative results that are in the same range that some of the most typical EFM setups. These results could be useful for an accurate treatment and understanding of the EFM signal in the characterization of thin films.

## II THEORETICAL BACKGROUND

The experimental setup that we are simulating here is composed by a tip and a sample with a complex structure. The tip has at least three different elements that must be taken into account to obtain quantitative results of the electrostatic interaction: the tip apex, the cantilever and the shape of the tip. The cantilever effect has been studied before[9] and its influence has been determined as a function of the different distances of the geometry. The shape of the tip and the tip apex are going to be simulated by the tip apex radius  $R$ , the tip length  $L_{tip}$ , the tip half-angle  $\theta$  and the tip-sample distance  $D$ . The tip has axial symmetry along the  $z$ -axis. The value  $z=0$  corresponds to the tip apex and  $z=a$  to the sample surface. The sample is composed by a thin film with thickness  $h$  and dielectric constant  $\epsilon_1$ . The thin film is placed over a dielectric substrate with thickness  $L$  and dielectric constant  $\epsilon_2$ . The substrate surface is placed at  $z=b$  (i.e.  $h=b-a$ ). The lower limit of the substrate is a grounded metallic plate placed at  $z=c$  (i.e.  $L=c-b$ ).

The Generalized Image Charge Method [14] (GICM), as well as other numerical methods that replace the tip by some charged elements inside [15][16], is a powerful tool that is able to make fast and accurate simulations that include all the elements of the tip and sample. The details of this method, including a three layers thin film sample have been described

---

Manuscript received April 17, 2012, Accepted December 11, 2012  
G. M. Sacha is with the Department of Informatics, Escuela Politécnica Superior, Universidad Autónoma de Madrid, Cantoblanco, Madrid, Spain.  
Copyright (c) 2012 IEEE. Personal use of this material is permitted. However, permission to use this material for any other other purposes must be obtained from the IEEE by sending a request to pubs-permissions@ieee.org .

elsewhere<sup>10</sup> and only a brief description is given here. Basically, the GICM can be understood by a method that includes the sample and tip shape in two steps. First, the electrostatic potential is calculated for a punctual charge in front of the thin film sample. Using cylindrical coordinates, the electrostatic potential at the region where the punctual charge is placed can be written as follows:

$$V_1 = \frac{q}{4\pi\epsilon_0 r} + \int_0^\infty \Phi(k) J_0(k\rho) e^{Kz} dk \quad (1)$$

where  $J_0$  are the first order Bessel functions,  $q$  is the value of the punctual charge,  $z$  is the vertical coordinate,  $\rho$  is the lateral coordinate and  $\Phi(k)$  are coefficients that must be obtained applying the electrostatic boundary conditions at  $z=a$ ,  $z=b$  and  $z=c$  ( $V_i=V_{i+1}$ ,  $\epsilon_i V'_i=\epsilon_{i+1} V'_{i+1}$ ). In the most general case, the coefficients take the following form:

$$\tilde{H}\Phi(K) = (C_{12} - e^{-2KL})e^{-2Kb} - C_1(1 - C_{12} - e^{-2KL})e^{-2Ka} \quad (2)$$

where

$$\tilde{H} = 1 - C_{12}C_1 e^{-2Kh} - (C_{12} - C_1 e^{-2Kh})e^{-2KL} \quad (3)$$

and  $C_1=(\epsilon_1-1)/(\epsilon_1+1)$ ;  $C_{12}=(\epsilon_1-\epsilon_2)/(\epsilon_1+\epsilon_2)$ . Once we know the coefficients, we are able to solve the problem and obtain the electrostatic potential by direct integration of equation 1.

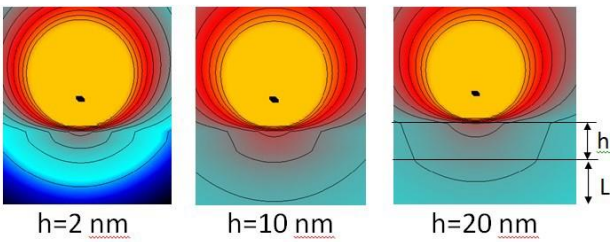
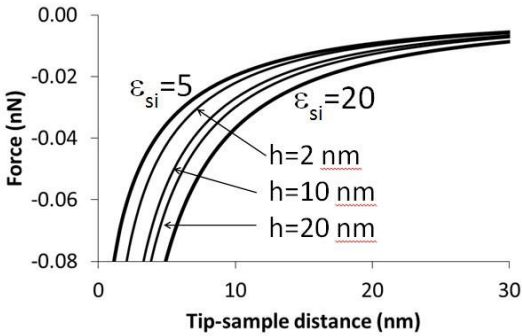


Fig 1. Electrostatic force between a spherical tip and a sample composed by a thin film with  $\epsilon_1=20$  over a substrate with dielectric constant  $\epsilon_2=5$ . The force is calculated for different values for the thin film thickness. The limits  $h=0$  and  $h=\infty$  corresponds to semiinfinite dielectric samples with  $\epsilon=5$  and  $\epsilon=20$  respectively. Equipotential lines for  $h=2, 10, 20$ nm are shown at the bottom of the figure.  $V=1V$ ,  $L=\infty$ ,  $R=25$ nm.

The second step of the GICM deals with the problem of including the shape of the tip in the simulation. To achieve this goal, the tip is discretized in a set of  $N$  points that will be used to fit the electrostatic potential. Furthermore, a set of  $N_c$  punctual charges and segments is included inside the tip. Since

both the tip shape and sample have axial symmetry, the charged elements inside the tip are placed along the  $z$ -axis. The values of the charges are calculated by a standard least-squares minimization routine or by the GICM<sub>f</sub> minimization[17] in the limit  $D \ll L$ . Once we know the value of the charges, the electrostatic force can be calculated by the interaction between the charge itself and the image charges obtained from  $V_1$  or from the derivative of the capacitance ( $F=(V^2/2)\partial C/\partial D$ ). It is worth noting that the potential applied to the tip  $V$  is proportional to the electrostatic force. For this reason, all the conclusions shown here can be applied for any  $V$  value. For simplicity, we have fixed  $V=1V$  in all the results shown in the article. Figure 1 shows some examples of the electrostatic force (top) and potential (bottom) between a spherical tip and a thin film sample. In this figure we can see the influence of the sample geometry on the electrostatic force. Due to the long-range nature of the interaction, the electrostatic force is still significantly different for thicknesses over 20nm, even when the tip-sample distance is smaller than 5nm. This is an evidence of the importance of the EFM elements that are far from the tip apex when the electrostatic interaction is being measured.

The best configuration of the GICM can be obtained by the winGICM software, which is powered by Artificial Neural Networks (ANNs)[14]. It is worth noting that this configuration is, in general, a different sum of charges that the one traditionally used by the standard image charge method[18] in simple configurations such as a sphere over a semiinfinite sample. However, the total amount of charge inside the tip is the same, independently of the sum of charges used to solve the problem. In the case of a thin film an additional condition must be included to get the GICM configuration by ANNs from the winGICM since their predictions comes from a realistic tip over a semiinfinite dielectric sample. To obtain the correct configuration, we have used a semiinfinite dielectric sample with the  $\epsilon$  value obtained by the average value of the dielectric constants of thin film ( $\epsilon_1$ ) and sample ( $\epsilon_2$ ). Without this optimization process, most of the results shown here are not easily affordable since the software configuration would have been done manually.

### III. INFLUENCE OF THE SAMPLE GEOMETRY

We are going to analyse the difference between two tips. The first one is a sphere with  $R=25$ nm. The second one is defined by  $R=25$ nm,  $L_{tip}=14\mu m$  and  $\theta=17.5^\circ$  (see inset of figure 2 for more details).

To study the influence of the sample, we are going to fix the dielectric constant of the substrate to  $\epsilon_2=5$ . The parameters that are going to be analysed will be the dielectric constant and thickness of the thin film ( $\epsilon_1$  and  $h$  respectively) and the thickness of the substrate ( $L$ ). In figure 1, we show the electrostatic force  $F$  vs  $D$  for the spherical tip over a sample where  $\epsilon_1=20$  and  $L \rightarrow \infty$ . For every  $h$  value, the force must be located in the window between the force of a semiinfinite dielectric sample with  $\epsilon_{si}=5$  (when  $h=0$ , the only contribution to the force comes from the substrate) and the force of a semiinfinite dielectric sample with  $\epsilon_{si}=20$  (when  $h \rightarrow \infty$  the contribution of the substrate vanishes). We also show in figure

1 the electrostatic potential distribution around the tip for  $h=2,10,20$  nm.

As we can see in figure 1,  $h$  is a parameter that has a strong influence in the force. For  $D < 5$  nm,  $F(h \rightarrow \infty)$  is at least two times bigger than  $F(h \rightarrow 0)$ . This difference makes EFM a good and accurate instrument to estimate  $h$ . However, we still do not know how accurate our simulations are to obtain quantitative results. The spherical tip is a simple model that has been used in several EFM applications giving good quantitative results [19]. However, most of these applications were related to metallic samples. It has been demonstrated before that this model is not adequate in general when dielectric samples are involved [8]. Previous results [20], [21] have even shown that there is a simple analytical expression that is useful to obtain the force between an EFM tip and a sample composed by a thin film over a metallic sample. This expression has been developed from the electrostatic force between an EFM tip and a metallic sample. In our case, we have a very different setup since the sample below the thin film is a dielectric.

We have calculated  $F$  for the realistic ( $F_{\text{tip}}$ ) and spherical tip ( $F_{\text{sp}}$ ) at  $D=1$  nm as a function of  $h$  (figure 2a) and  $\epsilon_1$  (figure 2b). In the figure we have included curves for several  $L$  values. Focusing on the limit  $L \rightarrow \infty$ , we can see in both figures a huge difference between  $F_{\text{tip}}$  and  $F_{\text{sp}}$ . Being  $F_{\text{sp}}$  the strongest interaction. Since the electrostatic force strongly decreases when the distance between charges increases, this effect is easy to understand since the tip is much bigger than the sphere. In the case of the sphere, the surface charge density is placed all around the tip, and the farthest side of the tip is at  $z=2R_{\text{tip}}$ . In the case of the realistic tip, the surface charge density is distributed between the tip apex and  $z=L_{\text{tip}}$ , which is a much bigger distance than  $z=R_{\text{tip}}$ .

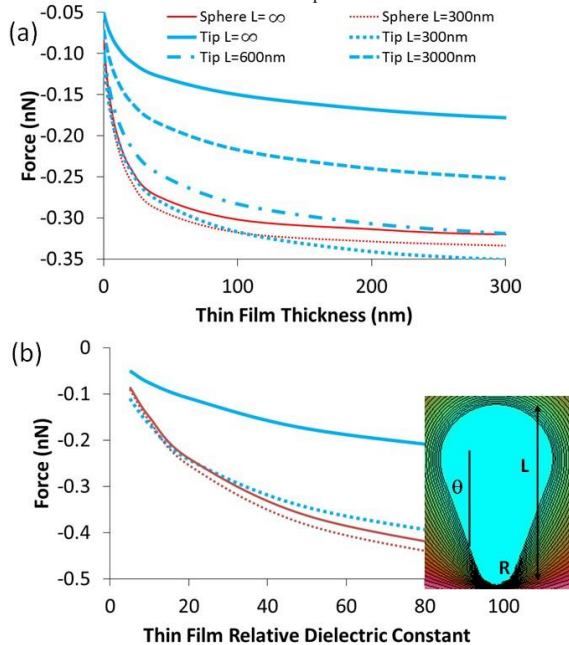


Fig 2. Electrostatic force as a function of the (a) thin film thickness  $h$  and (b) thin film relative dielectric constant  $\epsilon_1$  for different tips and geometries. In both cases  $V=1$  V,  $D=1$  nm,  $R=25$  nm and  $\epsilon_2=5$ . We fixed  $\epsilon_1=20$  in (a) and  $h=20$  nm in (b). The realistic tip is characterized by  $\theta=17.5^\circ$  and  $L_{\text{tip}}=14$   $\mu\text{m}$ . In both figures, the electrostatic force is shown for different distances of the grounded metallic plate.

Studying now the effect of smaller  $L$  values, we can see that the effect of the finite length of  $L$  affects in a different way  $F_{\text{sp}}$  and  $F_{\text{tip}}$ . The decreasing of  $L$  induces a significant increasing of  $F_{\text{tip}}$ . However,  $F_{\text{sp}}$  keeps constant as  $L$  decreases. This fact implies that the shape ( $L$  and  $\theta$ ) of the tip is the element that is related to the interaction between the tip and the metallic plate. Focusing on the curves where  $L=300$  nm, we see that the influence of the substrate thickness almost compensates the difference between  $F_{\text{sp}}$  and  $F_{\text{tip}}$ . This implies that a spherical tip over a thin film with  $L \rightarrow \infty$  could be a good model for the realistic tip over a thin film and a sample with  $L \approx 300$  nm. To use this model, however, we must take into account that the error increases in the limits where  $h \rightarrow \infty$  or  $\epsilon_1 \rightarrow \infty$ .

In figure 3 we show that, for the realistic tip, the influence of  $L$  is still strong when  $L=3$   $\mu\text{m}$ . This effect is due to the small convergence of the electrostatic force when the tip-sample distance increases. In this figure we show  $F$  vs  $D$  for very long  $D$  values (the sample has been restricted to the metallic plate, in order to isolate the influence of this element). The electrostatic force converges very fast for the sphere. For the realistic tips, however, the electrostatic force does not vanish until the tip-sample distance is as big as the tip length ( $\approx 14$   $\mu\text{m}$ ). To study in detail the relation between  $L_{\text{tip}}$  and  $L$ , we have shown in figure 3 the electrostatic force for a set of tips with different  $L_{\text{tip}}$ . In all the examples, the influence of the metallic plate does not vanish until  $D$  is at least two times bigger than  $L_{\text{tip}}$ . This result implies that in most of the typical EFM setups, the metallic plate will be a key parameter in the electrostatic interaction since usually  $L_{\text{tip}} > L$ .

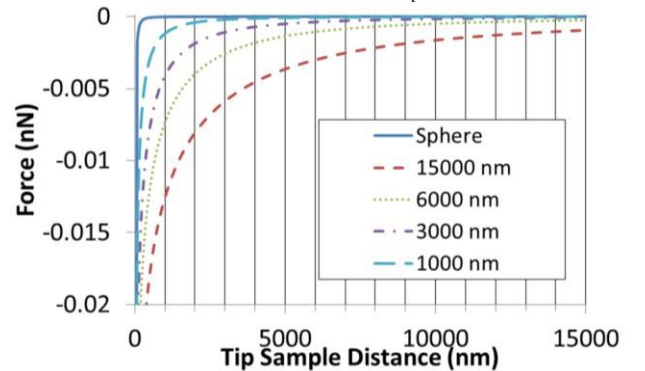


Fig 3. Electrostatic force for the spherical tip and realistic tips with different lengths. The sample is the metallic plate below the thin film and substrate and the tip-sample distance is referred here as the distance between the tip-apex and the metallic plate.  $R=25$  nm,  $V=1$  V and  $\theta=17.5^\circ$  for the realistic tips.

#### IV. INFLUENCE OF THE TIP SHAPE

At this point, we have studied in detail the influence of the sample geometry on realistic and spherical tips. We have also established that some changes in the sample geometry can strongly modify the electrostatic interaction, especially when realistic tips are included in the simulation. We have even demonstrated that the use of spherical tips as a numerical model gives adequate results for typical EFM samples. However, we have not studied in detail the influence of the tip parameters since, in the previous section, we have only included one EFM realistic tip.



In this section, we are going to extend our analysis to a wide variety of tips. Some experimental results on the analysis of the tip shape over thick films can be found on Refs [22][23]. In figure 4a we have represented the electrostatic force as a function of the thin film thickness for tips with lengths between  $L_{\text{tip}}=3\mu\text{m}$  and  $L_{\text{tip}}=20\mu\text{m}$ , and half-angles between  $\theta=17.5^\circ$  and  $\theta=35^\circ$ . In this figure we have fixed  $R=25\text{nm}$ . To include the effect of the tip radius, we have represented in figure 4b the electrostatic force for the tip used in the previous section ( $\theta=17.5^\circ$ ,  $L_{\text{tip}}=14\mu\text{m}$ ) and the spherical one with tip radius  $R=25, 50, 100\text{nm}$ . In all cases  $\epsilon_2=5$ ,  $\epsilon_1=20$  and  $V=1\text{V}$ .

We have found that the parameters of the tip interact in a complex way. For a tip with  $\theta=17.5^\circ$ , the effect of the tip length is always smaller than 20% between  $L_{\text{tip}}=3\mu\text{m}$  and  $L_{\text{tip}}=20\mu\text{m}$ . In this case, the tip length has a very small influence on the electrostatic interaction since it changes less than 20% when  $L_{\text{tip}}$  increases its value more than 6 times. However, in the case  $\theta=35^\circ$ , the electrostatic force can change up to 40% when  $L_{\text{tip}}$  changes from  $3\mu\text{m}$  to  $20\mu\text{m}$ . We can conclude that the influence of the tip length on the electrostatic interaction strongly depends on the half-angle of the tip. Finally, if we try to apply the spherical tip approximation, we find that it does not give accurate results for big  $\theta$  and  $L_{\text{tip}}$  values.

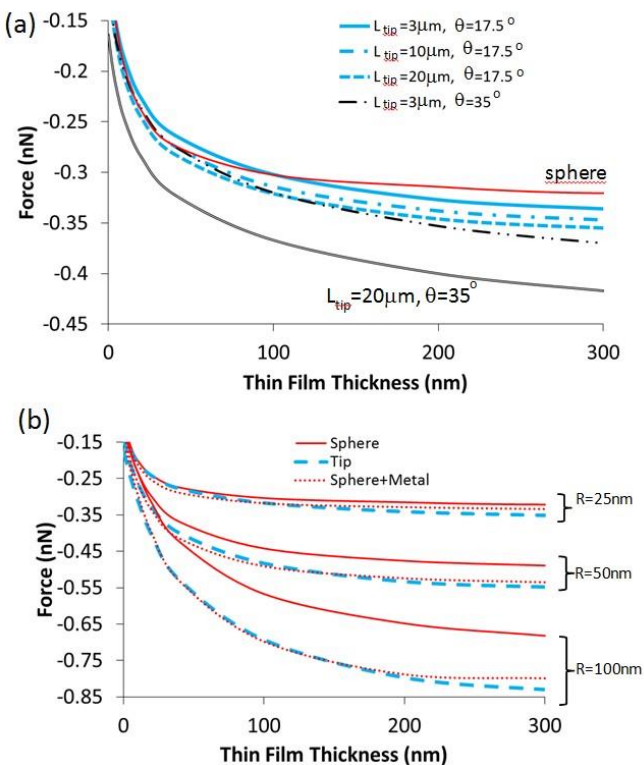


Fig 4. (a) Effect on the electrostatic force of the tip length and angle as a function as a function of the thin film thickness.  $R=25\text{nm}$  (b) Effect of the tip radius on the electrostatic force. Results are shown simultaneously for a realistic tip with  $L_{\text{tip}}=14\mu\text{m}$  and  $\theta=17.5^\circ$  and a spherical one.  $L+h=300\text{nm}$ ,  $\epsilon_1=20$ ,  $\epsilon_2=5$ ,  $V=1\text{V}$  in both figures.

Focusing now figure 4b we can see that the effect of the metallic plate for big  $R$  values changes the electrostatic force for both the realistic and spherical tips. As we can see in the figure, the influence of the metallic plate increases as  $R$

increases for the spherical tip. This effect can be easily understood if we remember that the shape of the tip is the key element in the interaction between the tip and the metallic plate. For the sample under study, the model of a spherical tip over a thin film without the metallic plate below the sample is not valid for tips with  $R>25\text{nm}$ . Although we cannot apply the simplest model suggested in the previous section, a spherical tip still gives accurate results for radius between  $R=25, 100\text{nm}$  including the metallic plate. Although this limitation makes the numerical calculations more difficult, we can still approximate the realistic tip by a spherical one, which is a great advantage since two parameters ( $L_{\text{tip}}$  and  $\theta$ ) are not included in the simulations.

## V CONCLUSIONS

In this paper we have demonstrated that EFM is a powerful tool to obtain a quantitative characterization of thin films. When the tip-sample distance is below 5nm, the electrostatic interaction can double its value for different thin film thicknesses. In order to obtain a quantitative characterization of the thin film geometry by EFM, we have analysed the influence of the shape of tip and sample on the signal, demonstrating that, in general, the electrostatic interaction is modified by EFM elements that are far from the tip apex.

We have shown that the thickness of the substrate below the thin film has a strong influence on the measurements done by realistic tips. The interaction due to a realistic tip increases when the substrate thickness decreases. This effect, however, is not present when a spherical tip is used as a numerical model (i.e. the interaction due to the sphere remains constant when we change the substrate thickness). On the other side, the constant interaction from the spherical tip is bigger than the one from the realistic tip in the limit where the substrate thickness tends to infinite. When we decrease the substrate thickness, we find that the interaction due to the realistic tip reaches similar values to the constant one from the sphere where the substrate thickness is around 300nm. In this limit, a system composed by a realistic tip, a thin film and a metallic plate can be replaced by a simple model composed by just a spherical tip and a thin film. Analysing in detail the effect of the shape of the tip, we found that this approximation is only valid when the tip radius is smaller than 25nm. For bigger values, the tip can still be simulated by a sphere, but the metallic plate below the substrate must be also included. We have demonstrated that physical magnitudes such as the surface charge density distribution and the size of the materials have a strong influence on the electrostatic force due to the interaction with the shape of the tip.

## ACKNOWLEDGMENT

Author acknowledges interesting discussion from J. J. Sáenz, C. Gómez-Navarro, J. Gómez-Herrero and E. Castellano-Hernández. This work was supported by TIN2010-19607. Author acknowledges support from the Spanish Ramón y Cajal Program.

## REFERENCES

- 
- [1] E. Bonarcurso, F. Schonfeld and H. J. Butt, "Electrostatic forces acting on tip and cantilever in atomic force microscopy," *Phys. Rev. B.*, vol. 74, pp. 085413, 2007
- [2] J. E. Jang, S. N. Cha, Y. Choi, D. J. Kang, D. G. Hasko, J. E. Jung, J. M. Kim, and G. A. J. Amaratunga, "A Nanogripper Employing Aligned Multiwall Carbon Nanotubes," *IEEE Transactions on Nanotechnology*, vol. 7, pp. 389-393, 2008
- [3] A. N. Morozovska, E. A. Eliseev and S. V. Kalinin, "The piezoresponse force microscopy of surface layers and thin films: Effective response and resolution function," *J. Appl. Phys.*, vol. 102, pp. 074105, 2007
- [4] J. Hu, X.-D. Xiao, and M. Salmeron, "Scanning polarization force microscopy: A technique for imaging liquids and weakly adsorbed layers," *Appl. Phys. Lett.*, vol. 67, pp. 476-478, 1995
- [5] R. Quintero-Torres, "A Model for the Self Structuring of Nanotubes in Titanium Oxide," *IEEE Transactions on Nanotechnology*, vol. 7, pp. 371-375, 2008
- [6] M. O. Jensen, "Periodically structured glancing angle deposition thin films," *IEEE Transactions on Nanotechnology*, vol. 4, pp. 269-277, 2005
- [7] S. Pisana, C. Zhang, C. Ducati, S. Hofmann and John Robertson, "Enhanced Subthreshold Slopes in Large Diameter SingleWall Carbon Nanotube Field Effect transistors", *IEEE Transactions on Nanotechnology*, vol. 7, pp. 458-462, 2008
- [8] S. Gómez-Moñivas, L. S. Froufe, A. J. Caamaño and J. J. Sáenz, "Electrostatic forces between sharp tips and metallic and dielectric samples" *Appl. Phys. Lett.*, vol. 79, pp. 4048-4050, 2001
- [9] G. M. Sacha and J. J. Sáenz, "Cantilever effects on electrostatic force gradient microscopy," *Appl. Phys. Lett.*, vol. 85, pp. 2610-2612, 2004
- [10] E. Castellano-Hernández, J. Moreno-Llorena, J. J. Sáenz and G. M. Sacha, "Enhanced dielectric constant resolution of thin insulating films by electrostatic force microscopy" *J. Phys.: Condens. Matter* vol. 24, pp. 155303, 2012
- [11] E. Castellano-Hernández and G. M. Sacha, "Ultrahigh dielectric constant of thin films obtained by electrostatic force microscopy and artificial neural networks," *Appl. Phys. Lett.* Vol. 100, pp. 023101, 2012
- [12] C. Riedel, A. Alegría, G. A. Schwartz, J. Colmenero and J. J. Sáenz, "Numerical study of the lateral resolution in electrostatic force microscopy for dielectric samples," *Nanotechnology* vol. 22, pp. 285705, 2011
- [13] G. Gramse, I. Casuso, J. Toset, L. Fumagalli and G. Gomila, "Quantitative dielectric constant measurement of thin films by DC electrostatic force microscopy," *Nanotechnology* vol. 20, pp. 395702, 2009
- [14] G. M. Sacha, F. B. Rodríguez, E. Serrano and P. Varona, "Generalized image charge method to calculate electrostatic magnitudes at the nanoscale powered by artificial neural networks". *Journal of Electromagnetic Waves and Applications* vol. 24, pp. 1145-1155 (2010)
- [15] A. N. Morozovska, E. A. Eliseev, G. S. Svechnikov, V. Gopalan and S. V. Kalinin, "Effect of the intrinsic width on the piezoelectric force microscopy of a single ferroelectric domain wall," *J. Appl. Phys.* vol. 103, pp. 124110, 2008
- [16] L. Tian, A. Vasudevarao, A. N. Morozovska, E. A. Eliseev, S. V. Kalinin et al, "Nanoscale polarization profile across a 180° ferroelectric domain wall extracted by quantitative piezoelectric force microscopy," *J. Appl. Phys.* vol. 104, pp. 074110, 2008
- [17] G. M. Sacha, "Method to calculate electric fields at very small tip-sample distances in atomic force microscopy," *Appl. Phys. Lett.* Vol. 97, pp. 033115, 2010
- [18] S. V. Kalinin, E. Karapetian, and M. Kachanov, "Nanoelectromechanics of piezoresponse force microscopy," *Phys. Rev. B* vol. 70, pp. 184101, 2004
- [19] G. M. Sacha, "Contrast and resolution of nanowires in Electrostatic Force Microscopy," *IEEE Transactions on Nanotechnology*, vol. 8, pp. 148-152, 2009
- [20] G. M. Sacha, E. Sahagún and J. J. Sáenz, "A Method for calculating capacitances and electrostatic forces in Atomic Force Microscopy," *J. Appl. Phys.*, vol. 101, pp. 024310, 2007
- [21] G. Gomila, J. Toset and L. Fumagalli, "Nanoscale capacitance microscopy of thin dielectric films," *J. Appl. Phys.* Vol. 104, pp. 024315, 2008
- [22] G. Gramse, G. Gomila and L. Fumagalli, "Quantifying the dielectric constant of thick insulators by electrostatic force microscopy: effects of the microscopic parts of the probe," *Nanotechnology*, vol. 23 pp. 205703, 2012.
- [23] L. Fumagalli, G. Gramse, D. Esteban-Ferrer, M. A. Edwards, and G. Gomila, "Quantifying the dielectric constant of thick insulators using electrostatic force microscopy," *Appl. Phys. Lett.* Vol. 96, pp. 183107, 2010

**Gómez-Moñivas Sacha** received the B.S. degree in Physics from Universidad Autónoma de Madrid, Madrid, Spain in 1999, the B. S. degree in Psychology from Universidad Nacional de Educación a Distancia, Madrid, Spain in 2003, and the Ph.D. in Physics from the Universidad Autónoma de Madrid, Madrid, Spain in 2003. He was a Postdoctoral Fellow at the Lawrence Berkeley National Laboratory, Berkeley CA and the Nanoscience Technology Center, Orlando, FL. He is currently a researcher at the Department of Computer Science, Universidad Autónoma de Madrid. His current research interests include artificial neural networks, models of sensory systems and thin films and their application to electronic devices.